# Communications

# Hyperhalogens: Discovery of a New Class of Highly Electronegative Species**

*Mary Willis, Matthias Götz, Anil K. Kandalam,* Gerd F. Ganteför,* and Puru Jena**

Electron affinity (EA), defined as the amount of energy necessary to remove an electron from an anion, plays a dominant role in reactivity. This is evidenced by halogen atoms, whose electron affinities are larger than those of any other element in the periodic table. However, there exists a class of molecules whose electron affinities are even larger. Bartlett and Lohmann were among the first to study such molecules nearly half a century ago. They showed that $PtF_6$ can even oxidize $O_2$ molecules[1] and Xe atoms.[2] Several years later, Gutsev and Boldyrev coined the term super-halogen to describe these highly electronegative species.[3] According to these authors, a superhalogen consists of a central metal atom surrounded by halogen atoms. When the number of these halogen atoms exceeds the maximal valence of the metal atom, the molecule possesses electron affinities that are much larger than that of the halogen atoms. In a series of subsequent theoretical studies, Boldyrev and co-workers showed that a large number of superhalogens, in which the central metal atom is typically an sp element, are possible.[4–8] The first photoelectron spectrum of $MX_2^-$ anions (M = Li, Na; X = Cl, Br, I) was reported by Wang and co-workers.[9] Subsequent photoelectron spectroscopic and theoretical studies have further confirmed the existence of superhalogens in the gas phase.[10–14] In a very recent theoretical study, it was proposed that the hydrogen atom can act as the central atom to form a superhalogen, and it was shown that the vertical detachment energies of $[H_nF_{n+1}]^-$ anions can be extremely high.[15] Numerous other super-halogen anions, such as permanganate ($MnO_4^-$),[16] perchlorate ($ClO_4^-$), hexafluorides ($AuF_6^-$ and $PtF_6^-$),[17–18] $BO_2^-$,[19] and $Mg_xCl_y^-$[20] have also been reported. In a joint experimental and theoretical study, we have presented unusually stable $Au_n(BO_2)$ clusters (n = 1–5) that exhibit superhalogen characteristics.[21] Because of their high EAs, superhalogens almost always exist as negative ions, usually as the anionic portions of salts. Because salts composed of superhalogens have highly oxidative properties, there is considerable interest in the synthesis of species with high EAs.

Herein we show that a new class of highly electronegative species can be synthesized if the peripheral halogen atoms are replaced by superhalogen moieties. We name this new class of electronegative species "hyperhalogens", because their electron affinities can even be larger than those of their super-halogen building blocks and thus can serve as ingredients in the synthesis of new superoxidizing agents.

Using density functional theory (DFT) and photoelectron spectroscopy (PES) experiments with a cluster beam, we demonstrate this possibility by concentrating on a gold atom and also a gold cluster decorated with $BO_2$ superhalogens. The $BO_2$ molecule, like $MnO_4$, has a large electron affinity of 4.32 eV,[19,21] whilst its anionic counterpart, $BO_2^-$, being isoelectronic with $CO_2$, is a very stable anion.

It has been shown recently that the EA of an $XF_n$ cluster (X = Cu, Ag, Au; n = 1–6) increases as the central coinage metal atom is decorated successively with fluorine atoms.[22,23] This happens as the extra electron is delocalized over several halogen atoms. We questioned whether the electron affinity would increase even further if the metal atom is decorated with superhalogen molecules instead. In this case, the extra electron will be delocalized over superhalogen moieties. What would happen if some but not all of the halogens atoms were replaced with superhalogen molecules; would the electron affinity lie in between the two? For example, would the electron affinity of $Au(BO_2)_2$ be much larger than that of $AuO_2$? Similarly, would the electron affinity of $AuO(BO_2)$ be in between that of $AuO_2$ and $Au(BO_2)_2$?

From our DFT-based calculations (Table 1), we found that the electron affinity of $Au(BO_2)_2$ is 5.54 eV, which is 1.6 times larger than that of $AuO_2$.[24] On the other hand, the electron affinity of $AuO(BO_2)$ is 4.21 eV, which lies between that of

[*] M. Willis, Prof. Dr. P. Jena
Department of Physics, Virginia Commonwealth University
Richmond, VA 23284 (USA)
Fax: (+1) 804-828-7073
E-mail: pjena@vcu.edu

M. Götz, Prof. Dr. G. F. Ganteför
Department of Physics, University of Konstanz
78457 Konstanz (Germany)
E-mail: gerd.gantefoer@uni-konstanz.de

Prof. Dr. A. K. Kandalam
Department of Physics, McNeese State University
Lake Charles, LA 70609 (USA)
E-mail: akandalam@mcneese.edu

*Table 1:* Experimental and calculated ADE and VDE of the $[Au_n(BO_2)]^-$, $[Au_nO(BO_2)]^-$, and $[Au(BO_2)_2]^-$ clusters.[a]

| Clusters | ADE [eV] | | VDE [eV] | |
|---|---|---|---|---|
| | exptl | theor. | exptl | theor. |
| AuO[24] | 2.378 | | 2.378 | 2.31 |
| AuO$_2$[24] | 3.40 | | 3.40 | 3.47 |
| Au(BO$_2$) | 2.8 | 3.06 | 3.0 | 3.34 |
| AuO(BO$_2$) | 4.0 | 4.21 | 4.4 | 4.42 |
| Au(BO$_2$)$_2$ | 5.7 | 5.54 | 5.9 | 5.66 |
| Au$_3$(BO$_2$) | 3.1 | 3.00 | 3.2 | 3.36 |
| Au$_3$O(BO$_2$) | 4.9 | 4.86 | 5.2 | 5.01 |

[a] ADE = adiabatic detachment energy, VDE = vertical detachment energy. The experimental uncertainty is ±0.1 eV.

$AuO_2$ and $Au(BO_2)_2$. These results are validated by our photoelectron spectroscopy measurements.

The fact that the electron affinities of superhalogens can be further enhanced by modifying the building blocks provides a new method for designing highly electronegative species. By suitably choosing the composition of these hyperhalogens and corresponding cations, new materials can possibly be designed and synthesized with unique properties. In the following we provide details of our computational and experimental results.

The electron affinity and vertical detachment energy (VDE) of AuO and $AuO_2$ have been determined earlier by experiment and theory.[24–27] According to the most recent work, AuO has an EA of 2.378 eV, and the VDE of $AuO^-$ is also measured as 2.378 eV, whilst calculations carried out at the CCSD(T) level gave a VDE of 2.312 eV.[24] We use these values for comparison with the corresponding values for $Au(BO_2)_n$ ($n = 1$–2) and $AuO(BO_2)$ clusters in Table 1.

We begin with a discussion of the electron affinity of AuO and $Au(BO_2)$. As the oxygen atom is replaced by $BO_2$ in AuO, the electron affinity of the resultant $Au(BO_2)$ cluster increases to 2.8 eV (Table 1). Similarly, a comparison of the VDE of $(AuO)^-$ and $[Au(BO_2)]^-$ clusters show that the replacement of oxygen with $BO_2$ results in an increase of 0.6 eV, from 2.378 eV to 3.0 eV, despite the fact that $Au(BO_2)$ is a closed-shell system whereas AuO is open-shell. Even though neither AuO nor $Au(BO_2)$ is a superhalogen, it is important to note that replacing an electronegative atom, oxygen, by a superhalogen, $BO_2$, leads to a significant increase in electron affinity. This will be shown to play a major role in our following discussion.

We next consider $AuO_2$ and $Au(BO_2)_2$ clusters. The latter is formed by replacing two oxygen atoms with two $BO_2$ superhalogen moieties. The electron affinity of $AuO_2$ was reported to be 3.40 eV which, as expected, is larger than that of AuO.[24] Strikingly, the electron affinity of $Au(BO_2)_2$ is 5.7 eV which is substantially larger than that of $AuO_2$ and $Au(BO_2)$ (see Table 1). Similarly, the VDE of $[Au(BO_2)_2]^-$ is 5.9 eV, whilst the VDE of $[AuO_2]^-$ is 3.40 eV. Given the fact that $BO_2$ behaves as a monovalent species, whereas oxygen is divalent, the question arises as to whether the comparison of the EA between $AuO_2$ and $Au(BO_2)_2$ is meaningful. To address this issue and allow a better comparison, we have considered monovalent species, namely halogens, as the ligands. We calculated the EA values of $AuX_2$ (X = F, Cl, Br, I) and compared them with that of $Au(BO_2)_2$ cluster. Note that in both $AuX_2$ and $Au(BO_2)_2$ the gold atom is in the same oxidation state. Our calculated EA values of $AuF_2$, $AuCl_2$, $AuBr_2$, and $AuI_2$ molecules are 4.84 eV, 4.63 eV, 4.46 eV, and 4.38 eV, respectively, which are in good agreement with previous experimental and theoretical studies.[28,29] The EA values of $AuX_2$ molecules are significantly smaller than that of the corresponding theoretical EA (5.54 eV) of the $Au(BO_2)_2$ cluster. We therefore term $Au(BO_2)_2$ as a hyperhalogen as its electron affinity is significantly increased upon replacing the peripheral oxygen atoms (in $AuO_2$) or halogen atoms (in $AuX_2$) with the superhalogen moiety, $BO_2$.

To gain further insight into the properties of the $Au(BO_2)_2$ hyperhalogen, we first discuss the ground state geometries of

its neutral and anionic configurations (Figure 1). We found two energetically degenerate structural isomers having *cis* and *trans* forms for both the neutral and anionic species. In these
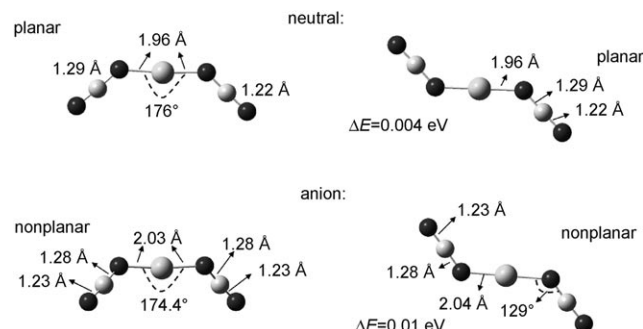


*Figure 1.* Geometries of the ground state and next-higher energy isomers of neutral and negatively charged $[Au(BO_2)_2]$ clusters. Au ●, B ●, O ●.

two isomers, the geometry of $BO_2$ moieties remains unaltered from its isolated state.[19,21] The neutral $Au(BO_2)_2$ cluster is an open-shell system, with a doublet ($2S + 1 = 2$) spin multiplicity. The natural bond orbital (NBO) charge analysis of the neutral cluster clearly showed that there is a charge transfer from the gold atom to both $BO_2$ moieties, resulting in a charge of $+0.92\,e$ on the gold atom and of $-0.46\,e$ on each of the $BO_2$ moieties. However, each $BO_2$ moiety requires one electron to be stabilized. Thus, the neutral $Au(BO_2)_2$ cluster lacks one electron, similar to that of a halogen atom.

The $[Au(BO_2)_2]^-$ cluster is a closed-shell system with a large HOMO–LUMO gap of 5.68 eV. The unusually large HOMO–LUMO gap, electronic shell closure, and the large binding energy of the extra electron (EBE or VDE) makes the $[Au(BO_2)_2]^-$ cluster a very stable anion that is ideal for forming a salt. The NBO charge analysis shows that the extra electron is delocalized over the entire cluster, thereby stabilizing both the $BO_2$ moieties and the entire $[Au(BO_2)_2]^-$ cluster. The VDE values of both isomers of the $[Au(BO_2)_2]^-$ cluster are calculated to be 5.66 eV and 5.62 eV, respectively. The PES of the $[Au(BO_2)_2]^-$ cluster obtained from our experiments is shown in Figure 2 and compared with that of
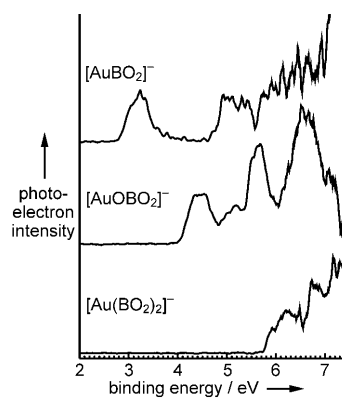


*Figure 2.* Comparison of photoelectron spectra of $[Au(BO_2)]^-$, $[AuO(BO_2)]^-$, and $[Au(BO_2)_2]^-$ clusters.

[Au(BO₂)]⁻ and [AuO(BO₂)]⁻. The experimental electron affinity of [(AuBO₂)₂] is estimated to be 5.7 eV, whilst the measured VDE of its anions is 5.9 eV. The calculated VDEs for both the isomers are in good agreement with the measured value (5.9 ± 0.1 eV) in Table 1. Therefore, the possibility that both these isomers could be present in the cluster beam cannot be ruled out. The enhanced stability of [Au(BO₂)₂]⁻ is thus reflected in the PES as large VDE and EA values. This is further confirmed by studying the thermodynamic stability of the Au(BO₂)₂ cluster, namely by calculating the energy required to fragment the cluster into smaller stable clusters. The binding energy of Au(BO₂)₂ measured with respect to Au(BO₂) and BO₂ is 2.09 eV. The binding energy of [Au-(BO₂)₂]⁻ measured with respect to Au(BO₂) and BO₂⁻ is 3.31 eV and with respect to [Au(BO₂)]⁻ and BO₂ is 4.57 eV. Thus, the hyperhalogen Au(BO₂)₂ not only possesses anomalously large electron affinity, but also has a very stable anion.

As gold can exist in an oxidation state of +3, it would be expected that Au(BO₂)₄ can also have larger electron affinity than, say, AuF₄. To examine this possibility, we computed the equilibrium geometries of neutral and anionic Au(BO₂)₄. Two nearly degenerate structures were found for the anionic Au(BO₂)₄; one having a cross shape and the other in the form where O-Au-O is bonded to a B₄O₆ structure. The vertical and adiabatic detachment energies of the former isomer are 7.13 eV and 7.10 eV, respectively. The electron affinity of AuF₄ is calculated to be 6.84 eV.[23] The cross-shaped structure is similar to the previously reported[30] Au(N₃)₄⁻ unit in ammonium tetraazidoaurate(III). The current experimental conditions did not permit us to synthesize this cluster owing to the low boron concentration in our PACIS source. We are currently redoing our measurements by introducing additional boron to the source. These results along with calculations will be published at a later date.

We now examine the structure and electron affinity of the AuO(BO₂) cluster, which is formed when one of the oxygen atoms of AuO₂ is replaced by a BO₂ molecule. The oxygen atom can either bind to gold, forming AuO(BO₂), or to BO₂, forming the Au(BO₃) cluster. The ground-state geometries of the neutral and anionic AuO(BO₂) cluster are shown in Figure 3 a,b, respectively. In both cases, the structure of the BO₂ moiety again remains intact and the oxygen atom binds to gold. However, the B-O-Au angle increased from 128° in the anion to 160° in the neutral species. The neutral AuO-(BO₂) cluster prefers a triplet (2S + 1 = 3) spin multiplicity, whilst the anion is a doublet (2S + 1 = 2). The singlet state (2S + 1 = 1) of the neutral AuO(BO₂) cluster is 1.34 eV higher in energy than the triplet state.

The PES of the [AuO(BO₂)]⁻ cluster is given in Figure 2. The calculated electron affinity of the AuO(BO₂) cluster is 4.21 eV, which agrees well with the experimental value of 4.0 eV. The first peak in the PES spectra of [AuO(BO₂)]⁻ is broad, which is due to the structural relaxation of the resultant neutral cluster as the extra electron is removed (see Figure 3 a,b). The calculated VDE, which corresponds to the transition from the anionic doublet to neutral triplet state, is 4.42 eV. This transition originates from the detachment of a β (spin-down) electron from the anionic doublet, thereby resulting in a triplet spin state. Our calculated VDE is in
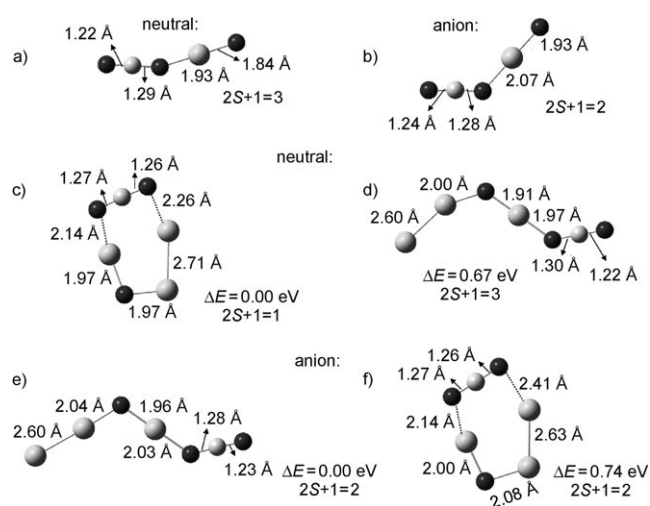


*Figure 3.* The geometries of neutral and negatively charged [AuO(BO₂)] and [Au₃O(BO₂)] clusters. Au ●, B ●, O ●.

excellent agreement with the measured VDE of 4.4 eV. The next-higher energy peak in the PES (in the range of 5–5.4 eV) corresponds to the electron detachment from a spin-down electron as well. Furthermore, the peak at about 5.6 eV in Figure 2 can be explained as originating from the transition from the spin doublet ground state of the anion to the spin singlet excited state of the neutral species. The calculated value for this transition is 5.98 eV. The fourth energy peak in the energy range of 6–7 eV is a combination of transitions to excited state neutral triplet and singlet states. As expected, the electron affinity of the AuO(BO₂) cluster is in between that of the corresponding values of AuO₂ and Au(BO₂)₂ clusters.

Finally, we have investigated whether a hyperhalogen can be created by manipulating the central metal core as we have shown we can do by replacing the peripheral halogen atoms by superhalogen moieties. This is accomplished by comparing the structure and properties of AuO(BO₂) and Au₃O(BO₂) clusters. In Figure 3 c–f, the geometries of the ground state and higher energy isomer of the neutral and anionic Au₃O-(BO₂) clusters are shown. In the neutral Au₃O(BO₂) cluster, the oxygen atom inserts into the Au₃ cluster, thereby forming an Au₂OAu segment, which in turn binds weakly to both the oxygen atoms of BO₂ moiety (see Figure 3 c). In the higher energy isomer (Figure 3 d, ΔE = 0.67 eV) a chain of Au-Au⁻O bonds is formed with oxygen bonding to the third gold atom, which in turn is bonded to the BO₂ moiety. Interestingly, the spin multiplicity of the lowest-energy isomer is a singlet (2S + 1 = 1), whilst the higher energy isomer prefers the triplet (2S + 1 = 3) spin state. The structure of Au₃O(BO₂) is entirely different from that of the isoelectronic boric acid (BO₃H₃) in which the boron at the center is attached to three oxygen atoms, which in turn are terminated with three hydrogen atoms. The ground-state geometry of the [Au₃O-(BO₂)]⁻ cluster (Figure 3 e) is not only different from that of its neutral counterpart, but it is identical to the higher energy isomer (Figure 3 d) of the neutral species. On the other hand, the higher energy isomer (ΔE = 0.74 eV) of the [Au₃O-

$(BO_2)]^-$ cluster (Figure 3 f) is identical to the ground state geometry of its neutral counterpart (Figure 3 c). Both these anionic isomers prefer a doublet $(2S+1=2)$ spin state. In both $AuO(BO_2)$ and $Au_3O(BO_2)$ clusters, the $BO_2$ moiety retains its structural identity. Moreover, the ground-state geometry of $[Au_3O(BO_2)]^-$ can be viewed as a $[AuO(BO_2)]^-$ cluster bound to a $Au_2$ unit.

The photoelectron spectrum of the $[Au_3O(BO_2)]^-$ cluster is given in Figure 4 and compared with that of $[Au_3(BO_2)]^-$. The introduction of an oxygen atom into the $[Au_3(BO_2)]^-$
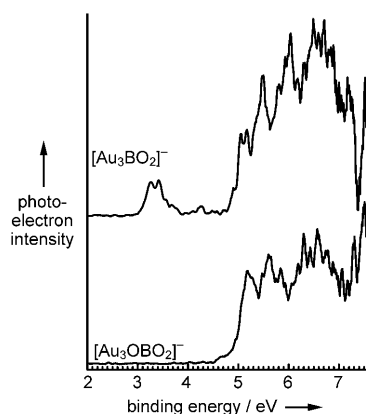


*Figure 4.* Comparison of photoelectron spectra of $[Au_3(BO_2)]^-$ and $[Au_3O(BO_2)]^-$ clusters.

clusters dramatically increases the electron binding energy (EBE) to anomalously large values of 5 eV and more. The fact that the $[Au_3O(BO_2)]^-$ cluster is an open-shell system (doublet spin multiplicity) makes this anomalous increase of EBE even more dramatic. Interestingly, changing the central metal core in $AuO(BO_2)$ to $Au_3O(BO_2)$ resulted in a significant increase in the adiabatic detachment energy (ADE) and VDE values of the cluster. The large differences in the neutral and anionic ground state geometries of the $Au_3O(BO_2)$ cluster are manifested in the PES data. Our calculated VDE of 5.01 eV, resulting from the transition of the anionic doublet state to the neutral triplet state, is in very good agreement with the experimental value of 5.2 eV. However, our calculated EA of 4.19 eV does not match with the experimental ADE of 4.9 eV. This is because the resulting neutral species does not automatically reach its ground-state structure, but rather remains in a higher energy isomer that is structurally similar to the anionic ground state when the electron is detached from the ground state anionic cluster in the PES experiments of $[Au_3O(BO_2)]^-$. In this process, the electron detachment results in the transition to the potential energy surface of the higher energy isomer that is identical to the ground-state anion but not the ground state of the neutral species. To verify this observation further we calculated the theoretical ADE as the energy difference between the ground state anion (Figure 3 e and the structurally identical higher energy neutral isomer (Figure 3 d). This value is 4.86 eV, which agrees very well with the experimental ADE (ca. 4.9 eV). The second peak in the PES (see Figure 4) originates from the transition of the spin doublet anion

ground state to the spin singlet neutral cluster having the anion geometry. This energy is calculated to be 5.72 eV, which again matches very well with the position of the second peak.

The anomalously large VDE and ADE values of $[Au_3O-(BO_2)]^-$ cluster can be explained from the NBO charge analysis. In the case of the neutral cluster (Figure 3 c), all three gold atoms lost charge to the oxygen atom and the $BO_2$ moiety, with the gold atom bound to both oxygen and $BO_2$, leading with a charge loss of $-0.881$ e. This charge transfer from gold atoms to two highly electronegative entities (O and $BO_2$) resulted in a total positive charge of $+1.396$ e on the gold atoms. In case of the $Au_3(BO_2)$ isomer, the total NBO charge on the three gold atoms was only $+0.791$ e,[21] whilst in the case of $AuO(BO_2)$ cluster, the total charge on the gold atom is $+0.952$ e. As expected, in the case of the anionic cluster, the extra electron is distributed mostly on the positively charged gold atoms, with a minority of charge going to the oxygen atom and the $BO_2$ moiety.

The distribution of the extra electron $(-0.762$ e$)$ over all the three gold atoms in $[Au_3O(BO_2)]^-$ resulted in a large binding energy of the extra electron, thus yielding large values of VDE and ADE. On the other hand, in the $[AuO(BO_2)]^-$ cluster, the extra electron is mostly localized on the gold $(-0.392$ e$)$ and the terminal oxygen $(-0.41$ e$)$ bound to gold, thereby resulting in ADE and VDE values lower than that of the $[Au_3O(BO_2)]^-$ cluster. The fact that the electron affinity of $Au(BO_2)$ and $Au_3(BO_2)$ are nearly the same (Table 1), whilst that of $Au_3O(BO_2)$ is about 1 eV larger than that of $AuO(BO_2)$ suggests that the central metal core may play a role in the design of hyperhalogens, but it is not universal.

In summary, we see that the electron affinity depends on the nature of the ligands on the metal atom. A superhalogen is created when the metal atom is surrounded by halogen/oxygen atoms and its electron affinity is larger than that of the constituent halogen atoms. In contrast, a hyperhalogen is created when the metal atom is decorated with superhalogens and its electron affinity is even higher than that of the constituent superhalogen. In some cases, replacing the central metal atom by a metal cluster also permits the electron affinity to increase. Similarly, by choosing different super-halogen building blocks with electron affinities larger than that of $BO_2$, hyperhalogens with even higher electron affinities can be achieved. It is also possible that if the central atom is a transition metal atom, the hyperhalogen can even carry a magnetic moment and the corresponding material could lead to a ferromagnetic insulator if these moments align in parallel. This work has demonstrated that a new class of highly electronegative species can be designed and synthesized by tailoring both the superhalogen building blocks and the central metal core.

### Experimental Section

PES was conducted by crossing a mass-selected beam of negative ions with a fixed-frequency photon beam and analyzing the energy of the resultant photodetached electrons. It is governed by the energy-conserving relationship $h\nu = EBE + EKE$, where $h\nu$ is the photon energy, EBE is the electron binding (transition) energy, and EKE is the electron kinetic energy. Our apparatus, which has been described

# Communications

previously,[31] consists of a pulsed-arc cluster-ion source (PACIS), a time-of flight mass spectrometer for mass analysis and mass selection, an $F_2$ excimer laser operating at 7.9 eV for photo-detachment, and a magnetic-bottle-type electron energy analyzer. The electrodes in the PACIS source are mounted in a boron nitride cube. When oxygen was added to the carrier gas from an additional pulsed valve, we observed a strong progression of boron-containing $Au_nO_m$ clusters along with the signals of the $Au_nO_m^-$ species. The boron nitride of the cube is eroded by the $O_2$-containing plasma. Without oxygen, no boron contamination is observed in the mass spectra. We saw no peaks associated with nitrogen, even though our mass resolution $m/\Delta m \approx 1000$ is sufficient to distinguish nitrogen from oxygen compounds.

The resulting anions were then subjected to extraction and mass analysis/selection. From the experimental photoelectron detachment data, the threshold energies and the vertical detachment energies can be estimated. The threshold energy is determined by fitting the signal increase at low binding energy to a linear function; the intersection of this line with the axis is taken as the threshold energy. If the change in the ground-state geometry between the anion and the neutral is not too large, the threshold energy can be compared to the calculated electron affinity (EA), which is the energy difference between the ground states of the anion and corresponding neutral species. If the geometry of anion and neutral species differs significantly, then the threshold energy is compared to the calculated adiabatic detachment energies (ADE). The vertical detachment energy (VDE) is taken as the binding energy of the first maximum at lowest binding energy.

Calculations were carried out using DFT and generalized gradient approximation (GGA) for the exchange-correlation energy functional. We used the B3LYP functional and 6-311 + + G(3df) basis set for B and O atoms, and the SDD basis for Au atoms, as implemented in the Gaussian 03 code.[32] The latter basis functions include scalar relativistic corrections. The equilibrium geometries of neutral and anionic $Au(BO_2)_2$, $AuO(BO_2)$, and $Au_3O(BO_2)$ clusters were calculated by optimizing various initial structures without any symmetry constraints. The stability of these clusters was confirmed by analyzing their normal mode frequencies, which are all positive.

[1] N. Bartlett, D. H. Lohmann, *Proc. Chem. Soc.* **1962**, 115–116.
[2] N. Bartlett, *Proc. Chem. Soc.* **1962**, 218.
[3] G. L. Gutsev, A. I. Bolydrev, *Chem. Phys.* **1981**, *56*, 277–283.
[4] G. L. Gutsev, A. I. Boldyrev, *Chem. Phys. Lett.* **1984**, *108*, 250–254.
[5] G. L. Gutsev, A. I. Boldyrev, *J. Phys. Chem.* **1990**, *94*, 2256–2259.
[6] A. I. Boldyrev, J. Simons, *J. Chem. Phys.* **1992**, *97*, 2826–2827.
[7] A. I. Boldyrev, W. Von Niessen, *Chem. Phys.* **1991**, *155*, 71–78.
[8] A. I. Boldyrev, J. Simons, *J. Chem. Phys.* **1993**, *99*, 4628–4637.
[9] X.-B. Wang, C.-F. Ding, L.-S. Wang, A. I. Boldyrev, J. Simons, *J. Chem. Phys.* **1999**, *110*, 4763–4771.
[10] A. N. Alexandrova, A. I. Boldyrev, Y.-J. Fu, X. Yang, X.-B. Wang, L.-S. Wang, *J. Chem. Phys.* **2004**, *121*, 5709–5719.
[11] B. M. Elliott, E. Koyle, E. , A. I. Boldyrev, X.-B. Wang, L.-S. Wang, *J. Phys. Chem. A* **2005**, *109*, 11560–11567.
[12] J. Yang, X.-B. Wang, X.-P. Xing, L.-S. Wang, *J. Chem. Phys.* **2008**, *128*, 201102.
[13] J. V. Ortiz, *Chem. Phys. Lett.* **1993**, *214*, 467.
[14] M. Sobczyk, A. Sawicka, P. Skurski, *Eur. J. Inorg. Chem.* **2003**, 3790–3797.
[15] S. Freza, P. Skurski, *Chem. Phys. Lett.* **2010**, *487*, 19–23.
[16] G. L. Gutsev, B. K. Rao, P. Jena, X. B. Wang, L.-S. Wang, *Chem. Phys. Lett.* **1999**, *312*, 598–605.
[17] O. Graudejus, S. H. Elder, G. M. Lucier, C. Shen, N. Bartlett, *Inorg. Chem.* **1999**, *38*, 2503–2509.
[18] M. K. Scheller, R. N. Compton, L. S. Cederbaum, *Science* **1995**, *270*, 1160–1166.
[19] H. J. Zhai, L. M. Wang, S. D. Li, L.-S. Wang, *J. Phys. Chem. A* **2007**, *111*, 1030–1035.
[20] I. Anusiewicz, *Aust. J. Chem.* **2008**, *61*, 712–717.
[21] M. Götz, M. Willis, A. K. Kandalam, G. F. Ganteför, P. Jena, *ChemPhysChem* **2010**, *11*, 853–858.
[22] Q. Wang, Q. Sun, P. Jena, *J. Chem. Phys.* **2009**, *131*, 124301–1/6.
[23] P. Koirala, M. Willis, B. Kiran, A. K. Kandalam, P. Jena, *J. Phys. Chem. C* **2010**, DOI: 10.1021/jp101807s.
[24] H. J. Zhai, C. Burgel, V. Bonacic-Koutecky, L.-S. Wang, *J. Am. Chem. Soc.* **2008**, *130*, 9156–9167.
[25] D. Stolcic, M. Fischer, G. Ganteför, Y. D. Kim, Q. Sun, P. Jena, *J. Am. Chem. Soc.* **2003**, *125*, 2848–2849.
[26] Q. Sun, P. Jena, Y. D. Kim, M. Fischer, G. F. Ganteför, *J. Chem. Phys.* **2004**, *120*, 6510–6515.
[27] T. Ichino, A. J. Gianola, D. H. Andrews, W. C. Lineberger, *J. Phys. Chem. A* **2004**, *108*, 11307–11313.
[28] D. Schröder, R. Brown, P. Schwerdtfeger, X.-B. Wang, X. Yang, L.-S. Wang, H. Schwarz, *Angew. Chem.* **2003**, *115*, 323–327; *Angew. Chem. Int. Ed.* **2003**, *42*, 311–314.
[29] B. Dai, J. Yang, *Chem. Phys. Lett.* **2003**, *379*, 512–516.
[30] T. M. Klapötke, B. Krumm, J.-C. Galvez-Ruiz, H. Nöth, *Inorg. Chem.* **2005**, *44*, 9625–9627.
[31] S. Burkart, N. Blessing, B. Klipp, J. Müller, G. Ganteför, G. Seifert, *Chem. Phys. Lett.* **1999**, *301*, 546–550.
[32] Gaussian 03, Revision C.02, M. J. Frisch et al., Gaussian, Inc., Wallingford CT, **2004**.